


A novel breakthrough in wrist-worn transdermal troponin-I-sensor assessment for acute myocardial infarction

Shantanu Sengupta ¹, Siddharth Biswal², Jitto Titus², Atandra Burman², Keshav Reddy³, Mahesh C. Fulwani⁴, Aziz Khan⁵, Niteen Deshpande⁶, Smit Shrivastava⁷, Naveena Yanamala³, and Partho P. Sengupta^{3,*}

¹Sengupta Hospital and Research Institute, Nagpur- 440033, Vidarbha (Dist), India; ²RCE Technologies, 2292 Faraday Avenue, Carlsbad, CA 92008, USA; ³Division of Cardiovascular Disease and Hypertension, Rutgers RobertWood Johnson Medical School, 125 Patterson St, New Brunswick, NJ 08901, USA; ⁴Shrikrishna Hrudayalay and Critical Care Center, Department of Cardiology, Dhantoli, Nagpur - 440010, Vidarbha (Dist), India; ⁵Department of Cardiology, Crescent Hospital and Heart Center, Dhantoli, Nagpur- 440010, Vidarbha (Dist), India; ⁶Department of Cardiology, Spandan Heart Institute and Research Center, Dhantoli, Nagpur- 440010, Vidarbha (Dist), India; and ⁷Department of Cardiology, Advanced Cardiac Institute Pt JNM Medical College, Raipur- 492009, Chattisgarh, India

Received 2 February 2023; revised 14 February 2023; online publish-ahead-of-print 6 March 2023

Aims

Clinical differentiation of acute myocardial infarction (MI) from unstable angina and other presentations mimicking acute coronary syndromes (ACS) is critical for implementing time-sensitive interventions and optimizing outcomes. However, the diagnostic steps are dependent on blood draws and laboratory turnaround times. We tested the clinical feasibility of a wrist-worn transdermal infrared spectrophotometric sensor (transdermal-ISS) in clinical practice and assessed the performance of a machine learning algorithm for identifying elevated high-sensitivity cardiac troponin-I (hs-cTnI) levels in patients hospitalized with ACS.

Methods and results

We enrolled 238 patients hospitalized with ACS at five sites. The final diagnosis of MI (with or without ST elevation) and unstable angina was adjudicated using electrocardiography (ECG), cardiac troponin (cTn) test, echocardiography (regional wall motion abnormality), or coronary angiography. A transdermal-ISS-derived deep learning model was trained (three sites) and externally validated with hs-cTnI (one site) and echocardiography and angiography (two sites), respectively. The transdermal-ISS model predicted elevated hs-cTnI levels with areas under the receiver operator characteristics of 0.90 [95% confidence interval (CI), 0.84–0.94; sensitivity, 0.86; and specificity, 0.82] and 0.92 (95% CI, 0.80–0.98; sensitivity, 0.94; and specificity, 0.64), for internal and external validation cohorts, respectively. In addition, the model predictions were associated with regional wall motion abnormalities [odds ratio (OR), 3.37; CI, 1.02–11.15; $P = 0.046$] and significant coronary stenosis (OR, 4.69; CI, 1.27–17.26; $P = 0.019$).

Conclusion

A wrist-worn transdermal-ISS is clinically feasible for rapid, bloodless prediction of elevated hs-cTnI levels in real-world settings. It may have a role in establishing a point-of-care biomarker diagnosis of MI and impact triaging patients with suspected ACS.

* Corresponding author. Tel: +(646) 531 2613, Fax: +732-418-8379, Email: partho.sengupta@rutgers.edu

© The Author(s) 2023. Published by Oxford University Press on behalf of the European Society of Cardiology.

This is an Open Access article distributed under the terms of the Creative Commons Attribution-NonCommercial License (<https://creativecommons.org/licenses/by-nc/4.0/>), which permits non-commercial re-use, distribution, and reproduction in any medium, provided the original work is properly cited. For commercial re-use, please contact journals.permissions@oup.com

Structured Graphical Abstract

Key Question

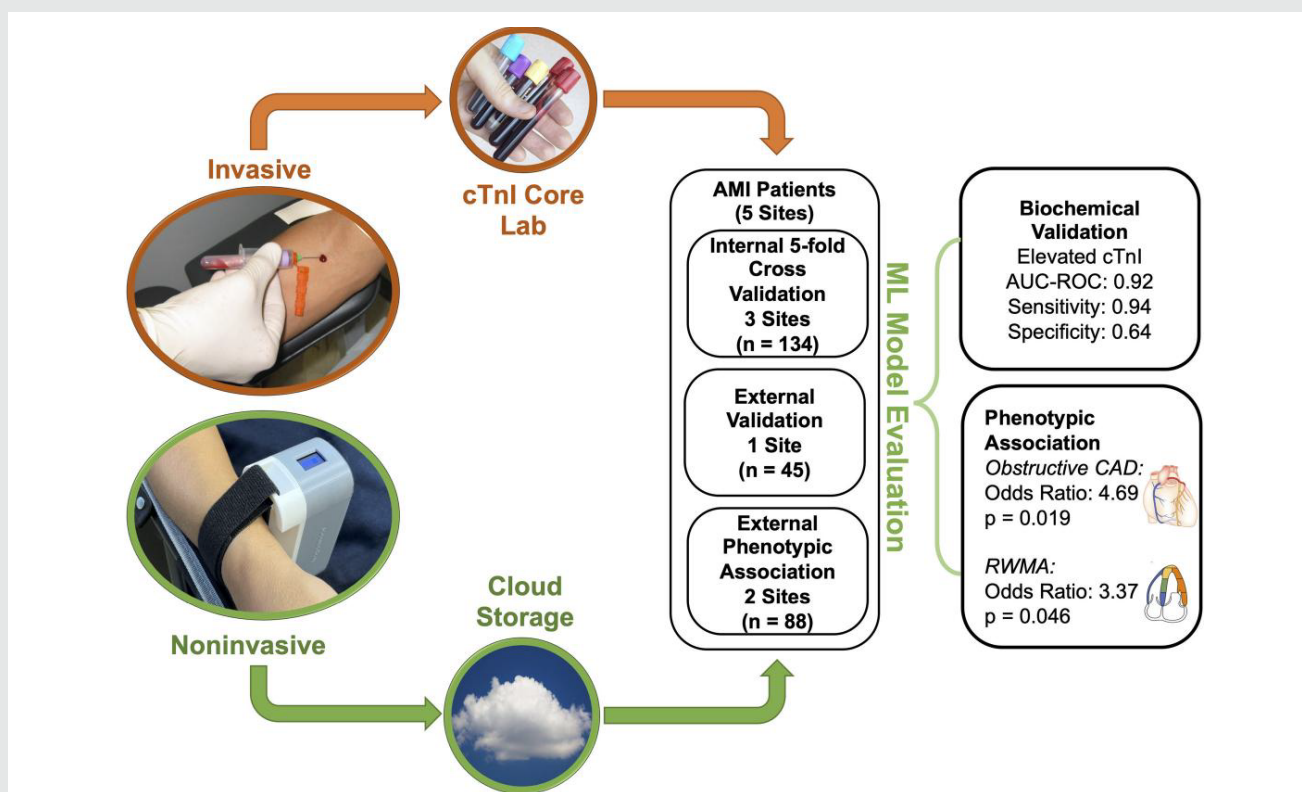
Can a wrist-worn transdermal infrared spectrophotometric sensor (transdermal-ISS) be utilized in real-world clinical settings for the bloodless estimation of elevated high-sensitivity cardiac troponin-I (hs-cTnI) levels?

Key Finding

In a multi-centre prospective study of patients presenting with acute coronary syndrome (ACS), a transdermal-ISS–derived deep learning model showed high diagnostic accuracy in predicting elevated hs-cTnI levels and was associated with left ventricular regional wall motion abnormalities and obstructive coronary artery disease.

Take Home Message

A transdermal-ISS for rapid bloodless estimation of hs-cTnI levels is feasible and may help establish a point-of-care (POC) biomarker diagnosis of acute myocardial infarction in patients with ACS.



The study evaluated a wrist-worn troponin-I sensor in hospitalized ACS patients with paired venous blood obtained for centralized troponin-I assay. A deep learning model was developed using the optical data from three training sites and externally validated for predicting elevated hs-cTnI (one site) levels and clinically associated with obstructive CAD and regional wall motion abnormalities (two sites).

Keywords

Acute myocardial infarction • Cardiac troponin-I • Infrared spectrophotometry • Deep learning

Introduction

Acute coronary syndromes (ACS) are the leading cause of mortality and morbidity worldwide and represent a spectrum of presentations ranging from unstable angina to acute myocardial infarction (MI).¹ In contemporary settings, symptom, or ECG-based differentiation of MI from unstable angina (~10% cases) or conditions mimicking ACS depends on biomarker demonstration of myocardial necrosis.^{2–4} Moreover, difficulties in early recognition of MI and delays in initiating effective evidence-based medical therapies can impact survival and quality of life.^{4–7}

Measurement of cardiac troponin levels, as a marker of myocyte necrosis, is routinely recommended in patients presenting with ACS, with blood draws required within a recommended turnaround time of 60 min.⁸ However, these turnover times for laboratory tests show wide variability and are challenging to implement in acute care settings confronted with staffing shortages and decreasing hospital resources.⁹ Specifically, overcrowding in emergency rooms can be associated with delays in blood sampling, overall diagnostic workup, and increased costs for assessing patients presenting with ACS.¹⁰

Innovations in sensor and computing technologies have led to increased adoption of smart wearable devices in cardiovascular medicine

for disease prevention, diagnosis, and management.¹¹ A potential solution to avoiding delay during symptoms of acute coronary artery occlusion is to implement a POC tool that confirms and accurately risk stratifies patients with suspected MI.¹² Although POC tests for estimating high-sensitivity cardiac troponin are available, currently, there are no hand-held devices approved for clinical use by the FDA. In this regard, we have recently reported the development of a novel wrist-worn transdermal infrared spectrophotometric sensor (transdermal-ISS) that can assess raised troponin-I levels based on infrared spectroscopy.¹³ Infrared spectroscopy can interrogate the material at the molecular level and is one of the cornerstones of analytical tools used to study structural and compositional chemistry.¹⁴ The most significant advantage is that a sensitive sensor can produce results within 5 min, without collecting blood and transferring the sample to the testing device. Although our preliminary laboratory and benchtop translational studies have provided initial feasibility data, the device has not been adequately evaluated in real-life clinical settings.

This multi-centre, observational study aimed to test the feasibility of implementing a remotely analysable, transdermal-ISS with machine learning analytics in the clinical setting for predicting elevated circulating high-sensitivity cardiac troponin-I (hs-cTnI) levels during a single time-point evaluation of patients hospitalized with ACS. Consenting and executing research for patients with ACS can be challenging, considering the need to implement the device for several minutes of recordings with a parallel blood draw while encountering confounding patient-related factors like stress, pain, the use of analgesics or sedatives, and time-sensitive therapies. Serum hs-cTnI levels increase within 3–4 h after the onset of symptoms and remain high for up to 4–7 days.¹⁵ We, therefore, sought a head-to-head comparison of hs-cTnI levels and transdermal-ISS recordings at a single random timepoint during the hospital stay after the patient was clinically stabilized to develop and validate deep learning models for predicting elevated hs-cTnI levels.

Methods

Study population

This study was an analysis of prospectively collected data from five centres in India (March 2022–November 2022) to train and test machine learning models based on the optical data derived from a molecular spectroscopic-based optical sensor device algorithm to predict the diagnosis of MI in patients presenting with the suspected ACS.¹² The development cohort comprised data from 3 sites, and the validation cohort comprised data from 2 locations (Figure 1).

The main inclusion criteria were patients admitted with new-onset chest pain and ischemic changes on the surface electrocardiography (ECG) suggestive of an ACS. Acute MI was defined clinically using ECG and the evidence of myocardial injury, manifested by a rising and/or falling pattern of cardiac troponin (cTn) values.¹⁶ MI was further categorized as ST-elevation MI (STEMI) based on typical symptoms and new ST segment elevation at the J point in more than two contiguous leads (>0.2 mV in V1 through V3 and >0.1 mV in other leads) or new left branch bundle block.¹⁷ In contrast, patients without ST segment elevation, with elevated cardiac troponin at presentation, were designated as non-ST-elevation MI (NSTEMI). Patients were defined to have unstable angina in the presence of chest pain resulting into hospitalization within 24 h of the most recent symptoms and absence of Hs-cTn elevation with one of the following: (i) ECG changes, (ii) regional wall motion abnormality on echocardiography, or (iii) angiographic evidence of CAD.^{7,18} In the absence of any of the above, an alternative diagnosis was sought based on the integrated clinical assessment. Patients with tattoos, scars, open wounds, or lesions that may interfere with the transdermal device, idiopathic pulmonary hypertension, implanted device, pregnancy, active malignancy, or refusing or an inability to provide informed consent were excluded. All study participants provided written informed consent, and the institutional ethics committee approved the study. All study procedures were performed in accordance with the declaration of Helsinki.

Study protocol

If eligible, informed consent was obtained, and the patient was enrolled only after initiating time-sensitive standard-of-care investigations and therapies so that the patient could comfortably undergo a transdermal-ISS recording. A detailed history, physical examination, a 12-lead ECG, and clinically indicated laboratory tests including troponin assays were recorded. The venous blood sample was taken within 15 min of optical data recording, one portion was processed locally for Hs-cTn measurement (at all five sites), and another portion (four sites) was sent for further hs-cTn assessment at a central laboratory. Patients at all five sites also underwent echocardiography and coronary angiography assessments as clinically indicated. A deep learning model was trained using transdermal-ISS data from 3 sites to predict elevated hs-cTnI levels (based upon central laboratory analysis). External validation of the deep learning model was performed for predicting elevated hs-cTnI (one site) levels and associated with angiographic and echocardiographic data (both external sites).

Clinical data collection

The following data were collected: basic demographics, risk factors for coronary artery disease including smoking history, comorbid conditions, physical findings, ECG findings, final diagnosis, and disposition. The length of stay was also recorded with diagnostics such as echocardiography, medications including thrombolysis, coronary angiography, percutaneous coronary interventions, or coronary artery bypass surgery. The discharged patients were followed up for one month through their clinical information system for revisits with cardiac symptoms or adverse clinical events (death and readmissions for cardiac reasons).

The data extracted from the echocardiography report consisted of the left ventricular ejection fraction (as calculated using Simpson's rule) and the presence of regional wall motion abnormalities (RWMA), assessed according to the American Society of Echocardiography guidelines) if identified in 2 contiguous segments in a coronary territory.¹⁹ The data extracted from the catheterization report consisted of the degree of stenosis visualized and type of intervention performed (e.g. balloon angioplasty and/or stent placement). Significant stenosis was defined in ≥ 1 major coronary artery (left main, left anterior descending, left circumflex, and right) at invasive coronary angiogram and defined as >50% reduction in lumen diameter.²⁰ The severity of each stenosis was further using a CASS-50 angiographic score since this score has a strong angiographic correlation with plaque burden.²¹

Endpoints

The primary endpoint of training the machine learning model was the presence of elevated troponin, as defined as a binary endpoint based upon central lab analysis (elevated vs. normal). The central lab utilized Abbott–Architect hs-cTnI assay with the use of the Architect system (Abbott Diagnostics), with an LoD of 0.01 ng/mL (10 ng/L), a 99th percentile cut-off point of 0.028 ng/mL (28 ng/L), and a coefficient of variation of <10% at 0.032 ng/mL (32 ng/L), as specified by the manufacturer. This analysis was utilized for training a machine learning model using transdermal-ISS data from 3 sites with external testing of the model performed one site. We also performed a secondary analysis to associate the transdermal-ISS–based prediction with the presence of RWMA on echocardiography and significant coronary artery disease for the data originating from two external sites, as defined in the previous sections.

Optical sensor data collection and analysis

A transdermal-ISS is a spectrophotometric device that functions based on an attenuated total internal reflection configuration. It non-invasively measures the infrared absorption corresponding to the troponin concentration in the system through the dermis. The detailed development of the device is outlined elsewhere.¹³ Briefly, our previous study included four phases of development. First, in an *ex vivo* exploratory work, we tested blood samples of patients ($n = 30$) with various cTnI levels on a research-grade attenuated total reflectance–based infrared spectrometer. The optical readouts representing the signature cTnI absorbance peaks were investigated and showed a positive linear correlation of 0.71. Subsequently, we developed the transdermal-ISS device and tested its ability to fit on the wrist in two cohorts of patients ($n = 9$ and $n = 24$) to assess the potential to classify

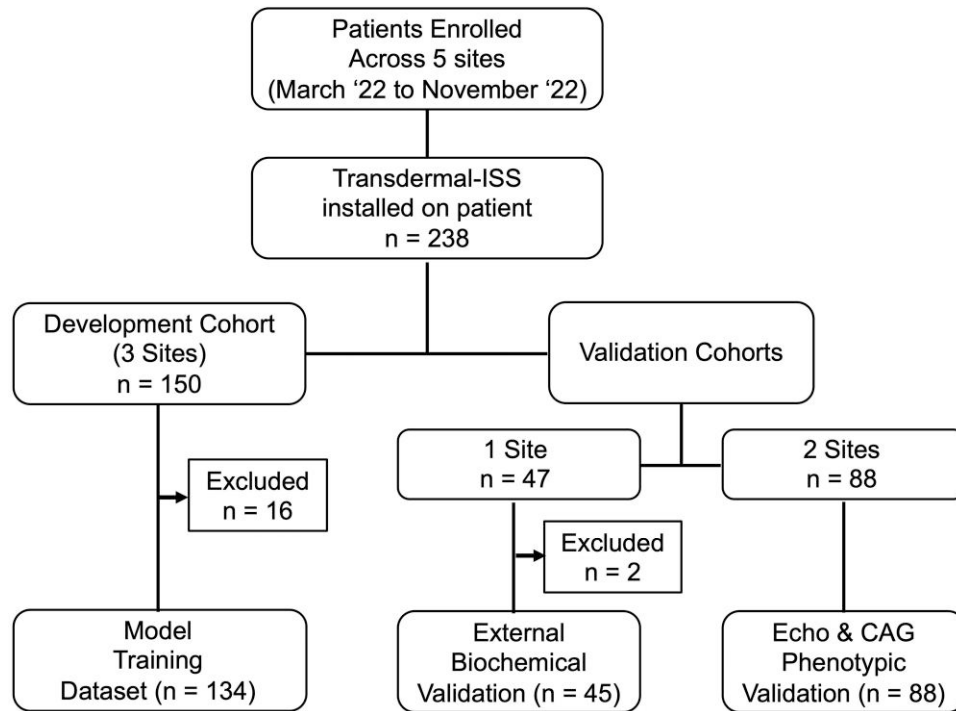


Figure 1 CONSORT diagram for clinical evaluation of the wrist-worn transdermal troponin-I-sensor. CONSORT, Consolidated Standards of Reporting Trials.

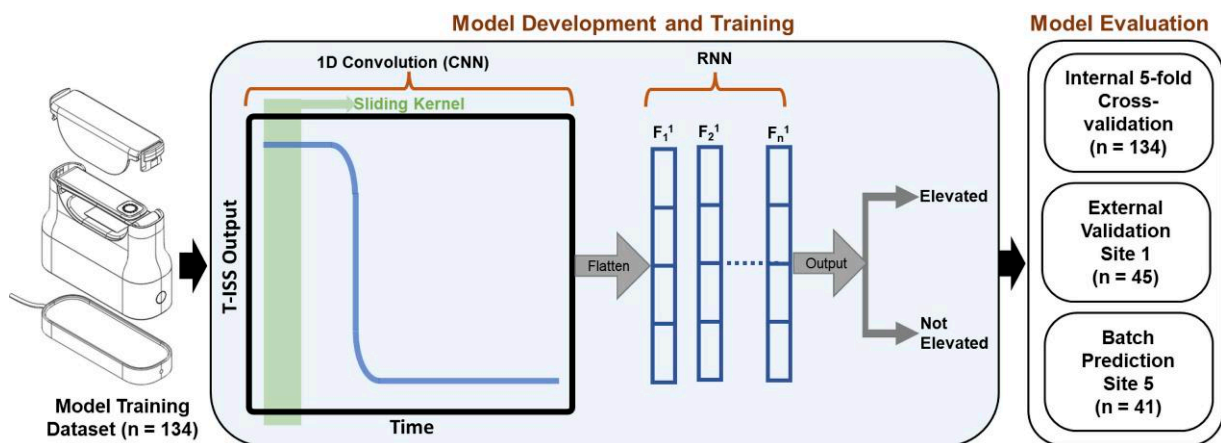


Figure 2 Deep learning framework. Schema representing a deep convolution neural network (CNN) architecture with recurrent neural networks (RNN) for detecting troponin using signalling data from a wrist-worn wearable sensor device.

patients with elevated troponins. This exploratory analysis revealed an area under the receiver operator characteristic curve of 0.85 with a sensitivity of 100% and specificity of 70.59%. We further tested a higher fidelity point of care device and in a controlled clinical setting and observed a positive linear correlation of 0.77 over a wide range of hs-cTnI concentrations. These steps subsequently form the basis of testing the device further in real-life settings in the present study.

A transdermal-ISS was used on recruited and consented patients to get an optical readout. First, the patient's volar aspect of the wrist is scrubbed

with a 70% alcohol wipe, following which the button is pressed on the optical device. After completion of the 45-second background, the device is strapped on the wrist with the sensor surface contacting the prepped portion of the wrist for 3 min. The transdermal-ISS is then removed while the data are wirelessly transmitted to the Amazon cloud. Following this, blood was drawn within 15 min of using the optical device to determine the ground truth troponin value with the Abbott–Architect STAT high-sensitivity assay. All optical data were further processed to segment and remove three electronic noise-related spikes occurring at the same locations

in the time series that are common for all data. They occur due to the change in driving voltage states for the emitter/detector pair and completely unrelated to the analyte measurement. Upon the unbiased removal of the spikes, the data are ingested by the machine learning algorithm without any further processing. The average infrared absorbance for training and test was $428\,475.5 \pm 23\,474.7$ and $398\,114.4 \pm 23\,618.1$ AU with a coefficient of variation of 5.6% and 7.4% respectively.

Machine learning model development & evaluation

A hybrid convolutional neural network–recurrent neural network (CNN-RNN) model was used to develop a classifier to distinguish between patients with and without elevated troponin levels using transdermal-ISS sensor data as input. While data collected from three different sites ($n = 134$; [Figure 1](#)—model training data set) were included in the final model development and internal evaluation using a cross-validation approach, an unseen cohort of patients ($n = 45$ patients, [Figure 1](#)—external validation data set) from the fourth site—not included during the model training—was included to evaluate the performance and generalizability of the developed model. The architecture for the proposed CNN-RNN model is illustrated in [Figure 2](#). Briefly, a CNN-RNN-based architecture combines the capabilities of convolutional neural networks (CNNs) to learn local patterns and features in the data using convolutional filters²² and recurrent neural networks (RNNs) that can process sequential data such as time series by using recurrent connections that allow the network to retain information from previous time steps.²³ While the CNN-RNN hybrid model applied a CNN to process and extract local features from the time series data, the RNN was used to capture the temporal dependencies between the time steps of the transdermal-ISS signalling data. Thus, the input for the proposed CNN-RNN model is the time series in a time window of size 20 from the optical sensor. Let the input time series be $X = [x_0, x_1, x_2, \dots, x_t, x_{t+1}, \dots]$, where $x_t \in R$ is the input at time point t . The CNN embedding layer is composed of multiple 1D convolutional layers, a max pooling layer, and batch normalization layers. The output of the CNN, a set of reduced-dimensionality features from the pooling layer, is then fed as input to the RNN, which processes the sequence of features and produces the final predictions. While ADAM optimization techniques were used to learn model parameters,²⁴ Bayesian optimization was adapted for hyperparameter tuning during cross-validation. A summary of the hyperparameters for the proposed CNN-RNN model is presented in [Supplementary material online, Table S1](#). Further details corresponding to the model development process and technical specifications of the CNN-RNN classifier are described in [Supplementary material online, e-Methods 1](#).

Statistical methods

We describe the algorithm performance in the test set by (1) visual inspection of a calibration curve to show how accurately transdermal-ISS estimates the likelihood of elevated troponins and by (2) the area under the receiver operating characteristic curve (AUC) to quantify how well the transdermal-ISS discriminated between those with and without elevated troponin. In addition, we compared diagnostic metric outputs from the algorithm (sensitivity, negative predictive value, specificity, and positive predictive value) for each patient with the metrics determined in the test set using the individual's prediction probability as a threshold (cut-off: 0.5). Differences between potential moderator effects of clinical covariates on the predictive accuracy were evaluated using Cochran's Q test for heterogeneity of the AUC across categories of a moderating variable. Between-group comparisons were conducted using Pearson's chi-square test (for the goodness of fit) or Fisher's exact test (for categorical variables) and Student's t -test (for continuous variables) after testing for normal distribution using the Kolmogorov–Smirnov test. Using our previous¹³ AUC for differentiating elevated troponins of 0.85 and 0.5 for a null hypothesis value, assuming that at least 70% of patients with suspected MI will have elevated troponin value, a sample size of at least 40 in the test set was estimated to provide 90% power, assuming an α -level of 0.05.

Logistic regression models were used to analyse associations between abnormal transdermal-ISS prediction and the presence of RWMA and significant CAD using the data from the two external test sites. The following covariates were *a priori* selected and included in the regression models as

adjustments for known confounders: age, sex, smoking, a history of CAD, diabetes, hypertension, body mass index (BMI), and dyslipidaemia. All covariates were first assessed for univariable associations, followed by multivariate modelling of significant predictors utilizing a stepwise backward elimination approach [MedCalc ver. 20.0.11 (MedCalc Software, Ostend, Belgium)]. The ML modelling was performed using Python 3.8 (Ljubljana, Slovenia). The AI model was developed by conforming to the JACC PRIME checklist.²⁵ Statistical significance was tested at a global type I error rate of 0.05.

Results

Baseline and clinical characteristics

The overall study cohort from the five different sites included 238 patients (mean age 55 ± 12 years and 77% males), of whom 136 (57%) presented with STEMI, 53 (22%) with nSTEMI, and 49 (21%) with unstable angina and others causes ([Table 1](#)). Coronary angiogram was performed in 223 (94%) patients, and obstructive CAD was present in 192 (86%). A total of 13 (6%) patients had MI with non-obstructed or normal coronaries (MINOCA). There was a higher prevalence of males ($P = 0.02$) and a lower prevalence of smokers ($P = 0.0003$) in the development cohort in comparison with the validation cohort ([Table 1](#)). Similarly, a higher prevalence of obstructive CAD and reduced left ventricular ejection fraction (<50%) was noted in the development cohort in comparison to the validation cohort ([Table 1](#), $P < 0.05$). Participants in the validation group were more frequently thrombolized; however, the total burden of patients receiving percutaneous coronary revascularization and coronary artery bypass surgery was similar in both groups. ([Figure 1](#)).

Model performance in predicting elevated troponins

The model was developed using participants from 3 sites ($n = 134$ after excluding patients with unmeasured cTnI; [Figure 1](#) and [Supplementary material online, Figure S1](#)) to develop and train a CNN-RNN-based hybrid deep learning model ([Figure 2](#)). The performance of the developed model as assessed by AUC plots, precision, recall, and other threshold evaluation metrics is shown in [Table 2](#) and [Supplementary material online, Figure S2](#). The trained model showed excellent performance by five-fold cross-validation in the training set with an AUC of 0.90 [95% confidence interval (CI), 0.84–0.94; sensitivity, 0.86; and specificity, 0.82] ([Figure 3](#)). Across the five-fold cross-validation, the AUC ranged from 84.3% to 94.8% with a mean of 90.4%. The model performance in the external validation data set ($n = 45$) demonstrated a similar performance with an AUC of 0.92 (95% CI, 0.80–0.98; sensitivity, 0.94; and specificity, 0.64), further suggesting the generalizability of the model to identify elevated hs-cTnI levels across independent cohort ([Figure 3](#) and [Table 2](#)). To overcome limitations imposed by fewer patients with non-elevated hs-cTnI levels, we developed additional models using under-sampling and over-sampling techniques (see [Supplementary material online, Table S2](#)). However, there was no change in model performance.

Putative moderation of the predictive performance

We investigated whether important clinical covariates are likely to influence the predictive performance of the transdermal-ISS machine learning model performance ([Table 3](#)). No variables demonstrated a statistically significant moderator-type association with the predictive performance of the transdermal-ISS-based machine learning model to predict elevated troponin-I. Considering the small sample size of the test set, we also investigated the predictive performance across the covariates in the developmental set. However, no significant

Table 1 Demographics and baseline characteristics of the study participants (including overall model development and validation cohort)

Variable	Overall	Development cohorts (3 sites)	Validation cohorts (2 sites)	P-value
n	238	150	88	
Patient demographics				
Age in years, (mean \pm SD)	54.9 \pm 12.2	55.3 \pm 12.0	54.2 \pm 12.7	0.46
Sex (M), n (%)	185 (77.7)	124 (82.7)	61 (69.3)	0.02 [§]
BMI, (mean \pm SD)	24.4 \pm 2.9	24.3 \pm 3.2	24.6 \pm 2.8	0.90
Risk factors, n (%)				
Diabetes	105 (44.1)	73 (48.7)	32 (36.4)	0.058
Hypertension	120 (50.4)	73 (48.7)	47 (53.4)	0.479
Smoking	60 (25.2)	26 (17.3)	34 (38.6)	0.0003 [§]
Hypercholestrolaemia	11 (4.6)	4 (2.7)	7 (7.9)	0.061
Clinical presentation				
STEMI, n (%)	136 (57.1)	87 (58.0)	49 (55.7)	0.727
NSTEMI, n (%)	53 (22.3)	32 (21.3)	21 (23.9)	0.651
Unstable angina/other, n (%)	49 (20.6)	31 (20.7)	18 (20.4)	0.969
Central laboratory assay, n				
	179	134	45	
Time to assay in days, (mean \pm SD)	1.3 \pm 1.0	1.4 \pm 1.0	1.2 \pm 0.9	0.07
Elevated cTnI, n (%)	137 (76.5)	106 (79.1)	31 (68.9)	0.162
Day of sampling	1.3 \pm 1.0	1.4 \pm 1.0	1.2 \pm 0.9	0.07
Echo, n				
	229	141	88	
LVEF < 50%, n (%)	101 (44.1)	70 (49.6)	31 (35.2)	0.033 [§]
RWMA, n (%)	175 (76.4)	102 (72.3)	73 (83.0)	0.066
Coronary angiogram, n				
	223	142	81	
Obstructive CAD, n (%)	192 (86.1)	128 (90.1)	64 (79.0)	0.021 [§]
MINOCA, n (%)	13 (5.8)	6 (4.2)	7 (8.6)	0.176
CASS SCORE-50				
0, n (%)	31 (13.9)	14 (9.9)	17 (21.0)	0.021 [§]
1, n (%)	104 (46.6)	68 (47.9)	36 (44.4)	0.620
2, n (%)	47 (21.1)	28 (19.7)	19 (23.5)	0.510
3, n (%)	34 (15.3)	28 (19.7)	6 (7.4)	0.014 [§]
4, n (%)	7 (3.1)	4 (2.8)	3 (3.7)	0.715
Interventions				
Thrombolytics, n (%)	28 (11.8)	3 (2.0)	25 (28.4)	$P < 0.0001^{\S}$
PCI, n (%)	129 (54.2)	81 (54.0)	48 (54.5)	0.933
CABG, n (%)	10 (4.2)	6 (4.0)	4 (4.5)	0.839

Values reported are counts (%) or mean \pm standard deviation (SD). The items in bold indicate the specific tests performed with their corresponding sample sizes.

cTnI, cardiac troponin-I; LVEF, left ventricular ejection fraction; RWMA, regional wall motion abnormalities; CAD, coronary artery disease; MINOCA, myocardial infarction with non-obstructive coronary arteries; PCI, percutaneous coronary intervention; CABG, coronary artery bypass surgery; CASS, coronary angiographic scoring systems.

[§] $P < 0.05$ using the chi-square test.

statistical heterogeneity was detected even in the training set (see [Supplementary material online, Table S3](#)).

Association between abnormal transdermal-ISS prediction and obstructive CAD

For the two external test sites, abnormal transdermal-ISS prediction was associated with obstructive CAD in unadjusted analyses [abnormal prediction: odds ratio (OR) 3.64, 95% CI (1.11–11.83), $P = 0.031$]. Moreover, after adjusting for sex and smoking, abnormal transdermal-ISS prediction remained significantly associated with the presence of obstructive CAD [OR 4.69 (1.27–17.26), $P = 0.019$]

([Table 4](#)). No significant association was seen between transdermal-ISS predictions, the number of vessels with obstructive CAD, or the severity of angiographic disease measured using the CASS-50 angiographic score. Abnormal transdermal-ISS prediction was also associated with the presence of RWMA [abnormal prediction OR 3.37, 95% CI (1.02 to 11.15), $P = 0.046$]. This association persisted even after adjustment of the presence of the underlying obstructive CAD [adjusted OR, 3.7500, 95% CI (1.16 to 12.07), $P = 0.026$].

Discussion

This investigation is the first multi-centre, real-world clinical evaluation of a wrist-worn device that utilizes mid-infrared (MIR) spectroscopy for

transdermal assessment of elevated hs-cTnI levels in patients hospitalized with ACS. The proposed algorithm comprises two key components (central illustration): an algorithm for signal processing, transmission, and feature extraction from a wrist-worn wearable device and a deep learning model to classify samples as clinically normal or abnormal based on a clinically recommended cut-off value of troponin-I. The principal findings of the study are as follows: (i) the recording of transdermal-ISS waveforms and the transmission of data over the web occurred accurately and confirms the feasibility of obtaining the optical-sensor readings in routine clinical settings; (ii) the machine learning models showed stability and high accuracy for detecting elevated troponin-I which differentiated patients with MI

from unstable angina and other causes; and (iii) the model prediction was associated with the presence of significant coronary artery disease on coronary angiography and the presence of regional wall motion abnormalities on 2D echocardiographic imaging. These data should inform the design of future clinical trials where optical sensor-based machine learning models can be further optimized for detecting myocardial injury and understanding potential underlying pathophysiology for each phenotype of troponin elevation.

Since the 1990s, cardiac troponin has been used as a biomarker to evaluate myocardial injury. While immunoassays are highly developed and accurate, they call for time-sensitive logistics coordination between the lab and the ordering providers for blood draws and sample transport. Point-of-care assays, like Abbott's iSTAT,²⁶ are now more widely available, but their low sensitivity may confound the accuracy of quick rule out algorithms.²⁷ While new strategies in using high-sensitivity immunoassays and microneedle patches are worthy of continued consideration, the alternate strategy evaluated in this study using MIR has been used previously for analysis of serum,²⁸ urine,²⁹ breath,³⁰ skin,³¹ and other bodily fluids. Infrared spectroscopy has since been used in food, drug, the environment, forensics, and, most significantly, the therapeutic area for diagnosing cancer³² and even cardiac care.^{14,33} In addition, complex MIR spectrometers have recently reduced their footprints to fit into tabletop portable devices like OceanInsight's MZ5. However, due to its footprint and significant sensitivity to mechanical vibrations, MIR is frequently restricted to ex vivo modalities. This study introduces one of the earliest POC devices that fit over the wrist yet can provide an objective associated with elevated blood hs-cTnI patients diagnosed or suspected to have MI. Moreover, unlike breathalyzers, bilirubinometers, and pulse oximeters, this device can be used free of Clinical Laboratory Improvement Amendments of 1988 (CLIA) regulations³⁴ because no bodily samples are required.

MIR spectroscopy fingerprints (2000–800 cm^{-1}) biological materials up to a finite depth determined by the wavelength and the refractive indices of the materials that the light passes through. The MIR light interacts with many proteins, cytokines, and amino acids in the epidermis, interstitial fluid, sweat, or sebum, considering the optical sensor surface placed under the wrist (palmar surface). We used troponin elevation

Table 2 Performance metrics of the CNN-RNN hybrid model for predicting whether the recorded transdermal-ISS signal represents elevated or non-elevated cTnI levels in the train and test sets using cross-validation and external validation, respectively

	Primary model	
	Train set (5-fold CV) <i>n</i> = 134	Test set (external validation) <i>n</i> = 45
AUC-ROC	0.90 (0.84–0.94)	0.92 (0.80–0.98)
F1-score	0.90 (0.87–0.93)	0.89 (0.81–0.96)
Accuracy	0.85 (0.81–0.90)	0.84 (0.73–0.95)
Specificity	0.82 (0.72–0.92)	0.64 (0.40–0.84)
Sensitivity (recall)	0.86 (0.80–0.91)	0.94 (0.87–1.0)
Precision (PPV)	0.95 (0.91–0.98)	0.85 (0.74–0.94)
NPV	0.60 (0.48–0.75)	0.82 (0.61–1.0)

AUC, area under the curve; ROC, receiver operating curve; PPV, positive predictive value; NPV, negative predictive value; CV, cross-validation.

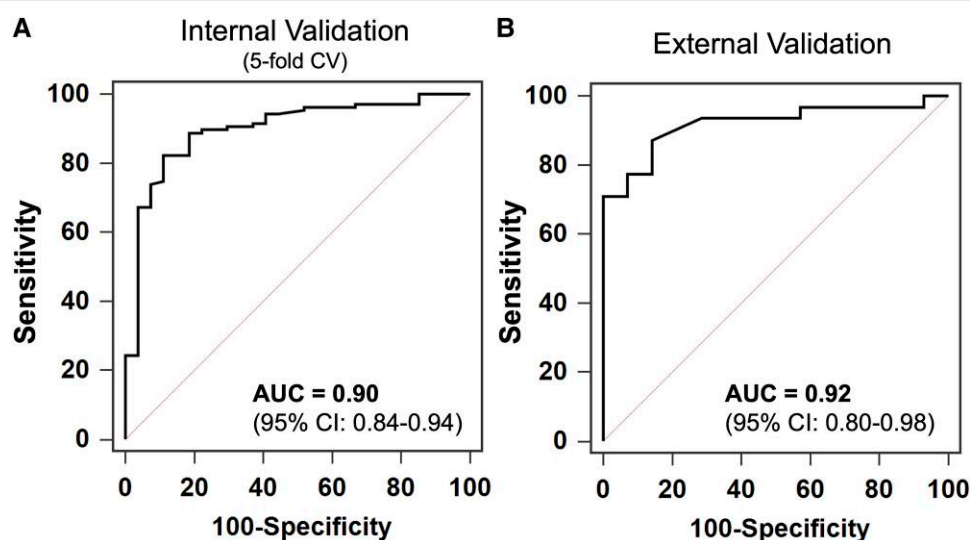


Figure 3 Model performance in the model training and external validation data sets. The receiver-operating characteristic curves demonstrate the performance of the CNN-RNN hybrid model in predicting elevated vs. non-elevated troponin levels in the (A) model training (five-fold cross-validation) and (B) external validation data sets.

Table 3 Evaluation of moderator effects on the diagnostic performance of transdermal-ISS to detect elevated troponin-I in the external validation cohort

Moderator variables and categories	n	AUC (95% CI)	Q (df) ^a	P _{het} -value
Overall	45	0.92 (0.79–0.98)	—	—
Age, years			0.88 (1)	0.34
<60	29	0.89 (0.72–0.97)		
≥60	16	0.96 (0.73–1.00)		
Sex			1.53 (1)	0.21
Male	27	0.96 (0.80–0.99)		
Female	18	0.83 (0.58–0.96)		
Obese (BMI ≥ 25 kg/m²)			0.96 (1)	0.32
Yes	10	0.82 (0.53–0.97)		
No	35	0.94 (0.79–0.99)		
Diabetes, hypertension, or dyslipidaemia			0.68 (1)	0.40
Yes	18	0.96 (0.75–1.00)		
No	27	0.90 (0.72–0.98)		
Smoking			NA	—
Yes	7	1.00 (0.59–1.00)		
No	38	0.90 (0.76–0.97)		
Significant CAD (>50%)			1.18 (1)	0.27
Yes	26	0.98 (0.84–1.00)		
No	14	0.75 (0.45–0.93)		

AUC, area under the curve; BMI, body mass index; CI, confidence interval; CAD, coronary artery disease.

^aCochrane's Q statistic of heterogeneity.

(higher than the 99th percentile value) as the gold standard—recommended method to diagnose ACS.¹² The transdermal-ISS device is designed to be sensitive largely to the wavelengths of interest for the detection of troponin.¹³ However, the exact nature of the biomarker [troponin T-I-C, binary complexes (I-C), free subunits (T and C), and fragments or related molecules thereof) tracked by the spectroscopy can be speculative. Moreover, co-presenting biomarkers such as CKMB, h-FABP, and NT-proBNP, albeit small, could contribute to the optical absorption window of hs-cTnI. Irrespective of the exact molecules tracked, one of the strengths of the study design was to use a centralized hs-cTnI assay to train the machine learning algorithm for predicting one-specific standardized threshold. The device's high accuracy in tracking elevated hs-cTnI levels, coupled with the ease of clinical application, suggests a potentially broader role of using this technology. Specifically, it may be implemented similarly to a single measurement of hs-cTn to facilitate the rapid diagnosis of ACS.³⁵ However, many factors impact troponin elevation and confound the clinical presentation, such as gender, age group, time of symptom onset, comorbidities, and biological variability.^{36,37,38} Although we performed subgroup analysis to investigate any potential moderator effect of clinical variables, further studies will be needed for a more in-depth understanding of the impact of these factors on device performance.

Besides the biological and clinical variabilities of circulating troponin, several device-related factors can impact the device's accuracy.

Specifically, implementing MIR spectroscopy has been complex since the efficiency of IR-based devices can be confused by stray light because the signal-to-noise ratio substantially affects the minimal detectable limit. This effect has been overcome by modulating the incoming light and sensitizing the detection system to the specific frequency of modulation, thus making it agnostic to ambient light. Compared with conventional spectrometers, the impact of mechanical vibrations has been greatly reduced by obviating any moving parts such as gratings or mirrors and replacing them with customized filters. Moreover, in pursuing a ubiquitous form factor solution, these devices can be susceptible to noise related to user errors. Some examples include sub-optimal and inconsistent contact between the wrist and sensor surface, which depends on the strap's tightness and the arm's steadiness during measurement. Another reason for signal occlusion is the insufficient cleaning of the wrist with alcohol wipes to help standardize the measurement site. We undertook a series of development to overcome these challenges during our clinical implementation. During several minutes of recording, noise related to motion and sensor–wrist contact quality may have contributed to the small coefficient of variation in infrared absorbance (5.6% and 7.4%) observed in the training and test sets, respectively. However, the binary ML classifier used in this study was adequate to address this range of variation in data. We have developed since then an algorithm which allows alerts to be provided for optimizing and repeating the recording. Future developments are underway to address development of the regression algorithm and addressing additional potential confounding effect of factors such as the wrist size, skin health, and melanin content to provide higher fidelity correlations with troponin levels.

Limitations and future directions

Several limitations of the study design are worth further consideration. First, this feasibility study enrolled patients hospitalized with ACS (including STEMI) and observed that a small fraction of patients had non-elevated hs-cTnI. While in contemporary practice, unstable angina represents a small cohort of ACS patients (~10%), its clinical differentiation from MI is clinically important.^{4,6,39} While under-sampling and over-sampling techniques showed that our machine learning model was stable, these data may be considered preliminary and hypothesis generating given the small sample size, population characteristics, and status of the technology. Future studies with larger sample size should address the diagnostic performance of the algorithm in chest pain units with a larger prevalence of normal hs-cTnI. Second, the diagnosis of acute myocardial injury requires a rise and/or fall of cardiac troponin on serial testing, which was not incorporated into the study design. The transdermal-ISS and the collection of a simultaneous additional blood sample for hs-cTnI measurement within 15 min of the recordings in the hospitalized patients after the standard of care assessments and diagnosis were established were critical for accessing standardized data for the model development and executing the research protocol without interrupting patient care. Since the device can be worn continuously to get a serial assessment, future studies would need to incorporate the device's potential use for serial measurements of cardiac troponin. Third, as stated previously, we utilized a ML-based binary classifier instead of regression for understanding the feasibility using the device in real-world settings. Finally, further developments need to address device and software settings to adapt to biological variability in disease, mechanical factors that impact data acquisition, and human factors that lead to performance variability.

Conclusions

The use of a transdermal-ISS for bloodless estimation of hs-cTnI shows the feasibility and may have a role in real-world settings for diagnosing

Table 4 Predictors of coronary artery luminal stenosis of >50% by unadjusted and adjusted logistic regression analyses of the test study population

CAD luminal stenosis > 50%	Univariable analyses			Multivariate analyses		
	OR	95% CI	P	OR	95% CI	P
	Age (years)	0.99	0.99–1.03	0.74	—	—
Male sex	4.37	1.42–13.39	0.009	5.03	1.49–16.95	0.009
Current smoker	6.83	1.44–32.33	0.015	—	—	NS
Body mass index (kg/m ²)	0.96	0.80–1.15	0.66	—	—	—
History of diabetes	1.40	0.44–4.47	0.56	—	—	—
History of hypertension	0.40	0.12–1.27	0.12	—	—	—
Abnormal transdermal-ISS prediction	3.64	1.11–11.83	0.031	4.69	1.27–17.26	0.019

Results were presented as unadjusted and adjusted odds ratios with 95% confidence intervals and P-values. Only covariates with a P-value < 0.05 for the association in the univariable model were included in the multivariate model.

NS, non-significant; OR, odds ratio; CI, confidence interval.

AMI in patients presenting with ACS. Future larger studies and pragmatic clinical trials would need to investigate the impact of transdermal-ISS on early, pre-hospital infarct diagnosis, triage, and therapy in emergency settings, including its utilization in emergency rooms, chest pain clinics, and implementation in ambulances and its utilization by trained paramedics.

Author contributions

P.S. and S.S. designed the study protocol. P.S., S.S., N.Y., and J.T. wrote the paper. S.B., P.S., J.T., and N.Y. performed the data analysis. S.S. oversaw the patient study at five sites. All authors contributed to editing the paper.

Supplementary material

Supplementary material is available at *European Heart Journal – Digital Health* online.

Acknowledgements

We thank Dr. Kunda Mungulmare and Jessie Katz for their help in the study coordination and data collection.

Conflict of interests: P.S. is an advisor to RCE Technologies and Echo IQ and holds option equity with these companies. S.B. holds option equity with RCE Technologies. N.Y. is an advisor to Turnkey Learning (P) Ltd. J.T. and A.B. are employees of RCE Technologies. All the other authors have nothing to disclose.

Data availability

The data that support the findings of this study are available on reasonable request to the corresponding author.

References

1. Wong ND. Epidemiological studies of CHD and the evolution of preventive cardiology. *Nat Rev Cardiol* 2014;**11**:276–289.
2. Shah AS, Anand A, Sandoval Y, Lee KK, Smith SW, Adamson PD, et al. High-sensitivity cardiac troponin I at presentation in patients with suspected acute coronary syndrome: a cohort study. *Lancet* 2015;**386**:2481–2488.
3. Collet J-P, Thiele H, Barbato E, Barthélémy O, Bauersachs J, Bhatt DL, et al. 2020 ESC guidelines for the management of acute coronary syndromes in patients presenting

without persistent ST-segment elevation: the task force for the management of acute coronary syndromes in patients presenting without persistent ST-segment elevation of the European Society of Cardiology (ESC). *Eur Heart J* 2021;**42**:1289–1367.

4. Puelacher C, Gugala M, Adamson PD, Shah A, Chapman AR, Anand A, et al. Incidence and outcomes of unstable angina compared with non-ST-elevation myocardial infarction. *Heart* 2019;**105**:1423–1431.
5. Anderson JL, Morrow DA. Acute myocardial infarction. *N Engl J Med* 2017;**376**:2053–2064.
6. Deckers J. Diagnostic re-classification and prognostic risk stratification of patients with acute chest pain. *Neth Heart J* 2019;**27**:575–580.
7. Kristensen AMD, Pareek M, Kragholm KH, Sehested TSG, Olsen MH, Prescott EB. Unstable angina as a component of primary composite endpoints in clinical cardiovascular trials: pros and cons. *Cardiology* 2022;**147**:235–247.
8. Vasani NM, Patel BD, Stanford BJ. Lean six sigma methodologies to reduce the cardiac troponin turnaround time in the core laboratory. *Lab Med* 2022:e0–e5.
9. Moskop JC, Sklar DP, Geiderman JM, Schears RM, Bookman KJ. Emergency department crowding, part 1—concept, causes, and moral consequences. *Ann Emerg Med* 2009;**53**:605–611.
10. Stoyanov KM, Biener M, Hund H, Mueller-Hennessen M, Vafaie M, Katus HA, et al. Effects of crowding in the emergency department on the diagnosis and management of suspected acute coronary syndrome using rapid algorithms: an observational study. *BMJ Open* 2020;**10**:e041757.
11. Bayoumy K, Gaber M, Elshafeey A, Mhaimeed O, Dineen EH, Marvel FA, et al. Smart wearable devices in cardiovascular care: where we are and how to move forward. *Nat Rev Cardiol* 2021;**18**:581–599.
12. Thygesen K, Alpert JS, Jaffe AS, Chaitman BR, Bax JJ, Morrow DA, et al. Fourth universal definition of myocardial infarction (2018). *Eur Heart J* 2019;**40**:237–269.
13. Titus J, Wu AHB, Biswal S, Burman A, Sengupta SP, Sengupta PP. Development and preliminary validation of infrared spectroscopic device for transdermal assessment of elevated cardiac troponin. *Commun Med* 2022;**2**:42.
14. Yang TT, Weng SF, Zheng N, Pan QH, Cao HL, Liu L, et al. Histopathology mapping of biochemical changes in myocardial infarction by Fourier transform infrared spectral imaging. *Forensic Sci Int* 2011;**207**:e34–e39.
15. Mahajan VS, Jarolim P. How to interpret elevated cardiac troponin levels. *Circulation* 2011;**124**:2350–2354.
16. Thygesen K, Alpert Joseph S, Jaffe Allan S, Chaitman Bernard R, Bax Jeroen J, Morrow David A, et al. Fourth universal definition of myocardial infarction (2018). *J Am Coll Cardiol* 2018;**72**:2231–2264.
17. Thygesen K, Alpert JS, Simoons ML, Chaitman BR, White HD, et al. Third universal definition of myocardial infarction. *Nat Rev Cardiol* 2012;**9**:620–633.
18. Diabetes Mellitus—Evaluating. Guidance for Industry. Center for Drug Evaluation and Research (CDER) 2008.
19. Lang RM, Badano LP, Mor-Avi V, Afilalo J, Armstrong A, Ernande L, et al. Recommendations for cardiac chamber quantification by echocardiography in adults: an update from the American Society of Echocardiography and the European Association of Cardiovascular Imaging. *Eur Heart J Cardiovasc Imaging* 2015;**16**:233–271.
20. Rosenthal RL. The 50% coronary stenosis. *Am J Cardiol* 2015;**115**:1162–1165.

21. Neeland IJ, Patel RS, Eshthardi P, Dhawan S, McDaniel MC, Rab ST, et al. Coronary angiographic scoring systems: an evaluation of their equivalence and validity. *Am Heart J* 2012;**164**:547–552.e541.
22. Krizhevsky A, Sutskever I, Hinton GE. ImageNet classification with deep convolutional neural networks. *Commun ACM* 2017;**60**:84–90.
23. Graves A. Generating sequences with recurrent neural networks. *arXiv preprint arXiv:1308.0850* 2013.
24. Kingma DP, Ba J. Adam: a method for stochastic optimization. *arXiv preprint arXiv:1412.6980* 2014.
25. Sengupta PP, Shrestha S, Berthon B, Messas E, Donal E, Tison GH, et al. Proposed requirements for cardiovascular imaging-related machine learning evaluation (PRIME): a checklist: reviewed by the American College of Cardiology Healthcare Innovation Council. *JACC Cardiovasc Imaging* 2020;**13**:2017–2035.
26. Apple FS, Ler R, Chung AY, Berger MJ, Murakami MM. Point-of-care i-STAT cardiac troponin I for assessment of patients with symptoms suggestive of acute coronary syndrome. *Clin Chem* 2006;**52**:322–325.
27. Collinson P. Cardiac biomarker measurement by point of care testing—development, rationale, current state and future developments. *Clinica Chimica Acta* 2020;**508**: 234–239.
28. Petrich W, Lewandrowski KB, Muhlestein JB, Hammond MEH, Januzzi JL, Lewandrowski EL, et al. Potential of mid-infrared spectroscopy to aid the triage of patients with acute chest pain. *Analyst* 2009;**134**:1092–1098.
29. Paraskavadi M, Morais CLM, Lima KMG, Ashton KM, Stringfellow HF, Martin-Hirsch PL, et al. Potential of mid-infrared spectroscopy as a non-invasive diagnostic test in urine for endometrial or ovarian cancer. *Analyst* 2018;**143**:3156–3163.
30. Selvaraj R, Vasa NJ, Nagendra SMS, Mizaikoff B. Advances in mid-infrared spectroscopy-based sensing techniques for exhaled breath diagnostics. *Molecules* 2020;**25**:2227.
31. Kastl L, Kemper B, Lloyd G, Nallala J, Stone N, Naranjo V, et al. *Mid-infrared spectroscopy in skin cancer cell type identification*. Novel Biophotonics Techniques and Applications IV: Optica Publishing Group; 2017. p1041305.
32. Hayashida M, Kin N, Tomioka T, Orii R, Sekiyama H, Usui H, et al. Cerebral ischaemia during cardiac surgery in children detected by combined monitoring of BIS and near-infrared spectroscopy. *Br J Anaesth* 2004;**92**:662–669.
33. Haas SL, Müller R, Fernandes A, Dzyek-Boycheva K, Würfl S, Hohmann J, et al. Spectroscopic diagnosis of myocardial infarction and heart failure by Fourier transform infrared spectroscopy in serum samples. *Appl Spectrosc* 2010;**64**:262–267.
34. Department of health and human services. Clinical laboratory improvement amendments of 1988. CFR 1988; 42:439.431-439.2001.
35. Than M, Cullen L, Aldous S, Parsonage WA, Reid CM, Greenslade J, et al. 2-Hour Accelerated diagnostic protocol to assess patients with chest pain symptoms using contemporary troponins as the only biomarker: the ADAPT trial. *J Am Coll Cardiol* 2012;**59**: 2091–2098.
36. Michel JB, Schussler JM. The trouble with troponin. *Proc (Bayl Univ Med Cent)* 2018;**31**: 238–239.
37. Apple FS, Fantz CR, Collinson PO; IFCC Committee on Clinical Application of Cardiac Bio-Markers. Implementation of high-sensitivity and point-of-care cardiac troponin assays into practice: some different thoughts. *Clin Chem* 2021;**67**:70–78.
38. Lan N, Bell DA. Revisiting the biological variability of cardiac troponin: implications for clinical practice. *Clin Biochem Rev* 2019;**40**:201–216.
39. Braunwald E, Morrow DA. Unstable angina: is it time for a requiem? *Circulation* 2013; **127**:2452–2457.